QUADRATIC EQUILIBRIUM ELEMENTS

E.A.W.Maunder & A.C.A.Ramsay
School of Engineering, University of Exeter,
North Park Road, Exeter, Devon, EX4 4QF, U.K.

SUMMARY

A new quadrilateral equilibrium element with quadratic stress fields is described for planar stress problems. The element is formulated as a superelement composed of four triangles using a force method which resolves the question of spurious kinematic modes. Numerical results for the single element are presented from an initial investigation aimed at determining the optimum internal arrangement.

1. INTRODUCTION

Stress based equilibrium elements have long had their exponents [1,2,3,4,5] with the aim of enabling dual analyses to be made. While this is still desirable, the demand for such elements now extends to error estimators [6,7] and limit analyses [8,9]. Part of the challenge of this type of element is that greater ingenuity is generally required for element formulation compared with the conventional displacement element. Stress fields may be defined to be fully continuous, or in a piecewise sense with minimal continuity for equilibrium. Element connection variables may be defined to represent stress fields as stress functions, or traction distributions on element sides. A potential problem with these elements is the existence of spurious kinematic modes. One solution is to block such modes at the element level by appropriate assembly of elements into a "superelement". This is common practice in models of aeronautical structures with shear panels and stiffeners. In the modelling of structural continua families of elements have been proposed [2], e.g. quadrilateral elements formed by four triangles based on subdivision of the quadrilateral by its diagonals. This latter technique is generalised in this paper with an arbitrary subdivision into four triangles when quadratic stress fields are used. Conjugate force and displacement variables are taken to represent distributions of normal and tangential tractions and displacements along element sides. These are shown in Figure 1, and are based on Legendre polynomials as defined in Table 1.

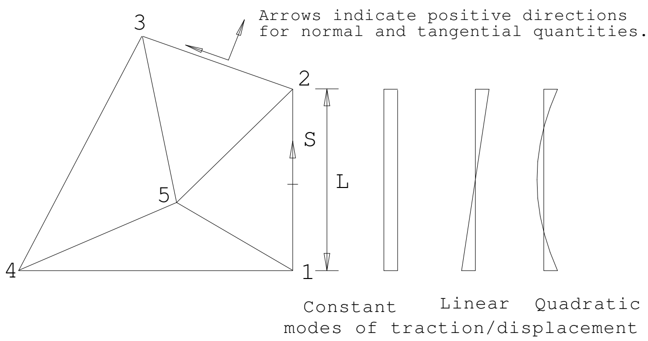

Figure 1: Superelement with modes of side traction and displacement.

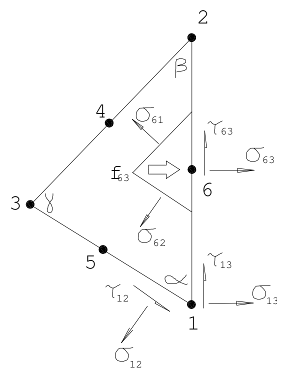

Figure 2: Stress components for a triangle.

Unit modes of traction			Unit modes of displacement		
Constant (g_0)	Linear (g_1)	Quadratic (g_2)	Constant (q_0)	Linear (q_1)	Quadratic (q_2)
$\frac{1}{tL}$	$\frac{12s}{tL^3}$	$\frac{60}{tL^3}\left(\frac{6s^2}{L^2}-\frac{1}{2}\right)$	1	s	$\frac{L^2}{12}\left(\frac{6s^2}{L^2}-\frac{1}{2}\right)$

Table 1: Unit modes of normal and tangential traction and displacement for element of thickness t .

2. SPURIOUS KINEMATIC MODES.

2.1 Single element.

There are twelve quadratic stress fields which are in equilibrium with zero body forces in plane stress. For a polygonal region "i " six modes of traction on each side are required to equilibrate with such internal stress fields. The independent side tractions $\{\bar{g}\}_i$ are given by the equation

$$[e]_i\{\beta\}_i = \{\bar{g}\}_i \ , \tag{1}$$

where $\{\beta\}_i$ represents the independent stress fields. The dimensions of $[e]_i$ are 15x12 and 21x12 for a triangle and quadrilateral respectively. Conjugate displacements $\{\bar{q}\}_i$ and deformations $\{\delta\}_i$ quantities are related by the contragredient transformation

$$[e]_i^T\{\bar{q}\}_i = \{\delta\}_i \ . \tag{2}$$

Spurious kinematic modes are represented by displacements $\{\hat{q}\}_i$ which satisfy the homogeneous form of Equation (2). These displacements have no corresponding stresses or tractions. In the language of vector spaces , spurious kinematic modes belong to the nullspace of $[e]_i^T$, and a basis for this space forms an orthogonal complement $[c]_i$ to $[e]_i$, i.e.

$$[e]_i^T[c]_i = [0]. \tag{3}$$

From the point of view of tractions, these are admissible when they can be derived from a $\{\beta\}_i$. Thus admissible tractions must satisfy

$$[c]_i^T\{\bar{g}\}_i = [c]_i^T[e]_i\{\beta\}_i = \{0\}, \tag{4}$$

and these equations represent generalised "release" conditions [10] for an element. The triangle and quadrilateral thus have 3 and 9 independent spurious kinematic modes/generalised releases respectively. Identification of these modes generally requires analysis of $[e]_i$, and may for example utilise singular value decomposition (SVD) which effectively enables the bases for $\{\beta\}_i$ and $\{\bar{g}\}_i$ to be transformed so that $[e]_i$ becomes diagonal.

2.2 Assembly of elements

When elements are assembled, spurious kinematic modes may propagate through the system. The consequences as regards admissible loads can be analysed in various ways. For a system of four triangular elements it appears "natural" to proceed with a force method as follows. Equilibrium equations for a "regular" model are formed as

$$\underset{60\text{x}1}{\{\bar{g}\}} = \underset{60\text{x}21}{[G]}\underset{21\text{x}1}{\{L\}} + \underset{60\text{x}\alpha}{[B]}\underset{\alpha\text{x}1}{\{p\}} \ , \tag{5}$$

where $\{\bar{g}\}$ contains the traction modes on all four elements, $\{L\}$ contains the independent traction loads on the bounding sides of the assembly, and $\{p\}$ contains α parameters representing self-equilibrating tractions in the absence of loads. The columns of $[G]$ and $[B]$ contain particular and complementary solutions respectively. The term "regular" is applied when no element releases are assumed to be present. With quadratic traction modes the statical indeterminacy α of the regular model is 15. The conjugate displacements $\{\bar{q}\}$ are compatible if they satisfy

$$[B]^T\{\bar{q}\} = \{0\}. \tag{6}$$

Now, simultaneous spurious kinematic modes $\{\hat{q}\}$ for the set of triangles can be written as

$$\{\hat{q}\} = \underset{60\text{x}12}{[C]}\{s\} \ , \tag{7}$$

where $[C]$ contains the submatrices $[c]_i$ on its diagonal, and $\{s\}$ represents an arbitrary combination of modes for the separate triangles. However, for the assembled triangles these must be compatible, and $\{s\}$ must satisfy

$$[M]\{s\} = \{0\}, \text{ where } [M] = [B]^T[C]. \tag{8}$$

Hence spurious kinematic modes exist in the system when the nullspace of $[M]$ is non-trivial. When releases are accounted for, admissible tractions must satisfy the homogeneous equations

$$[C]^T\{\overline{g}\} = \{0\} \text{ie.} [M]^T\{p\} + [C]^T[G]\{L\} = \{0\}. \tag{9}$$

Thus the statical indeterminacy of the system is reduced to $(\alpha - \overline{r})$ where $\overline{r}$ is the rank of $[M]$. It is found that generally $\overline{r}$ is 12, $(\alpha - \overline{r})$ is 3, and no spurious kinematic modes exist. However in the particular case when diagonals are used to subdivide the quadrilateral, $\overline{r}$ is 11, $(\alpha - \overline{r})$ is 4, and one spurious kinematic mode exists. This is restricted to the interfaces of the system, and consequently there are no constraints on the side tractions $\{L\}$.

3. STRESS FIELDS AND A FLEXIBILITY MATRIX.

The superelement is analysed with arbitrary subdivision, and SVD of $[M]$ is used to automate the analysis when the rank of $[M]$ is not fixed. Whence

$$[M] = [U][\Sigma][V]^T = [U_1 \mid U_2]\left[\begin{array}{c|c} \Sigma_1 & 0 \\ \hline 0 & 0 \end{array}\right][V]^T, \tag{10}$$

where $[\Sigma_1]$ contains the $\overline{r}$ non zero singular values of $[M]$, and $[U_1]$ has $\overline{r}$ columns. Equation (9) is transformed to

$$[\Sigma]^T\{\overline{p}\} + [V]^T[C]^T[G]\{L\} = \{0\}, \text{or } [\Sigma_1]^T\{\overline{p}_1\} = -[V]^T[C]^T[G]\{L\}, \tag{11}$$

where parameters $\{\overline{p}\} = [U]^T\{p\}$, and $\{\overline{p}\}$ is partitioned into $[\overline{p}_1 \mid \overline{p}_2]^T$ where $\{\overline{p}_1\}$ has dimension $\overline{r}$. Thus application of the complementary solution $\{p\} = [U_1]\{\overline{p}_1\}$ leads to an admissible particular solution $\{\overline{g}^0\}$ defined by

$$\{\overline{g}^0\} = [\overline{G}]\{L\}, \text{ where } [\overline{G}] = [I - BU_1\Sigma_1^{-1}V^TC^T][G]. \tag{12}$$

Admissible complementary solutions $\{\overline{g}^1\}$ are formed from $\{\overline{p}_2\}$ which has dimension $(\alpha - \overline{r})$

$$\{\overline{g}^1\} = [\overline{B}]\{\overline{p}_2\}, \text{ where } [\overline{B}] = [B][U_2]. \tag{13}$$

Stress fields in each triangle are now uniquely defined from admissible tractions as functions of $\{L\}$ and $\{\overline{p}_2\}$, and these fields are denoted by

$$\{\sigma^0\} = [S^0]\{L\}, \text{and } \{\sigma^1\} = [S^1]\{\overline{p}_2\}. \tag{14}$$

For a given set of loads, the stresses are still indeterminate, and are finalised by imposing weak compatibility conditions which also minimise the strain energy with respect to $\{\overline{p}_2\}$

$$\underbrace{\left[\int_V [S^1]^T[D]^{-1}[S^1]dV\right]}_{[F_{11}]}\{\overline{p}_2\} + \underbrace{\left[\int_V [S^1]^T[D]^{-1}[S^0]dV\right]}_{[F_{10}]}\{L\} = \{0\} \tag{15}$$

where $\{\sigma\} = [D]\{\varepsilon\}$. These equations for $\{\overline{p}_2\}$ lead to the following form of the superelement flexibility matrix

$$\underbrace{[F]}_{21\text{x}21} = [F_{00}] - [F_{10}]^T[F_{11}]^{-1}[F_{10}], \text{ where } [F_{00}] = \left[\int_V [S^0]^T[D]^{-1}[S^0]dV\right]. \tag{16}$$

4. SPECIAL RELATIONS FOR A TRIANGLE.

The three sided nature of triangular elements enables direct construction of some of the matrices involved in Sections 2 and 3, in particular the spurious kinematic mode matrix $[C]$ and the stress recovery matrices $[S^0]$ and $[S^1]$. Formally these depend on analyses of the matrices $[e]_i$ for each triangle. However explicit formation of $[e]_i$ is unnecessary. $[c]_i$ is obtained from three independent generalised release conditions by observing the following: at each corner normal and tangential stresses produced by tractions $\{\overline{g}\}_i$ must satisfy the equations of rotational equilibrium, e.g.

$$(\tau_{13}+\tau_{12})+(\sigma_{13}-\sigma_{12})\cot\alpha=0 \quad (17)$$

for corner 1 in Figure 2. In the pair of subscripts "ij", "i " refers to a node, and " j " refers to the direction normal to a side of a triangle. For the purposes of stress recovery it is convenient to refer to six nodes of a triangle : three at the corners and three at midsides. Quadratic stress fields are then recovered from admissible tractions in two stages represented by

$$\underset{3x1}{\{\sigma\}_i}=\underset{3x18}{[N]}\underset{18x15}{[P]_i}\underset{15x1}{\{\bar{g}\}_i} \quad (18)$$

where $[P]_i$ recovers stresses at the six nodes, and $[N]$ interpolates with the standard quadratic shape functions for a triangle. Stresses at the corners are immediately obtained from the normal and tangential components as appear in Equation (17). However at the midside nodes normal and tangential tractions only provide two of the three components required. The third components at these three nodes are determined by imposing the local equilibrium conditions that body forces normal to the sides, such as f_{63} in Figure 2, be zero. In this way the coefficients of $[P]_i$ are all found explicitly. For the construction of $[P]_i$, and the integrals in Equations(15) and (16) advantage is taken of local systems of axes and stress components peculiar to a triangle. These components are normal stresses in directions normal to the three sides of a triangle. This is a convenient variation on the "natural" stress components used by Argyris [11]. In this case the stress-strain matrix has the form

$$[D]=\frac{E}{(1-\nu^2)}\begin{bmatrix}1 & \cos^2\gamma+\nu\sin^2\gamma & \cos^2\beta+\nu\sin^2\beta\\ \cos^2\gamma+\nu\sin^2\gamma & 1 & \cos^2\alpha+\nu\sin^2\alpha\\ \cos^2\beta+\nu\sin^2\beta & \cos^2\alpha+\nu\sin^2\alpha & 1\end{bmatrix} \quad (19)$$

Integrations of coefficients in Equations(15) and (16) are carried out "exactly" and very simply using area coordinates for the stress fields $\{\sigma\}_i$.

5. NUMERICAL RESULTS FOR A SUPERELEMENT.

The geometry of an element is defined by 5 nodes, 4 corners and an internal node 5 common to all the triangles of the subdivision, see Figure 1. SVD of $[M]$ returns 12 singular values of which one may be theoretically zero. The threshold used for computed zero values was taken as $10^{-6}\times$ maximum singular value. A zero singular value was then observed when node 5 was specified to be within about $h\times10^{-6}$ of the intersection of the diagonals, where the dimension h represents the size of the element.

The formulation of the element response to tractions was tested by applying tractions consistent with statically and kinematically admissible stress fields to an arbitrarily shaped element, with node 5 in an arbitrary position. This is in the nature of a patch test, and the correct response was achieved. In particular a single element returns the correct solution for a rectangular cantilever beam loaded with parabolic shear as in Figure 3(a) [12]. Side displacements are shown diagrammatically in Figure 3(b) based on the displacement components in Table 2. For side 4 components q_{n0}, q_{n1}, and q_{t0} are prescribed with zero values, whereas q_{n2} and q_{t1} are computed to be zero. It should be noted that these displacements only give up to the quadratic components of the actual cubic displacements (the truth but not the whole truth!). The solution, being correct, is independent of the position of node 5. However for arbitrary tractions, the solution does depend on the position of node 5.

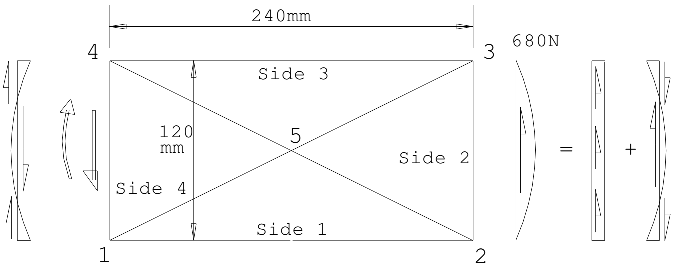

$t = 1mm;\ E = 207\times10^3\ N/mm^2\ ;\ \nu = 0.25$

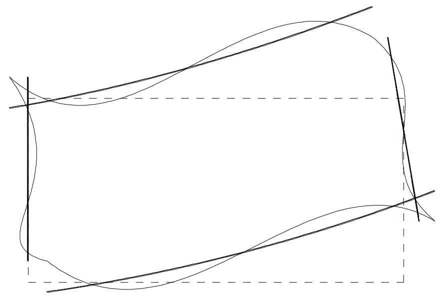

(a) Cantilever with parabolic shear modelled with one superelement. (b) Diagrammatic view of side displacements, discrete lines indicate quadratic forms returned by the element flexibility matrix.

Figure 3: Timoshenko's beam problem.

Side	Conjugate side displacements $\times10^3$					
	q_{n0}	q_{n1}	q_{n2}	q_{t0}	q_{t1}	q_{t2}
1	-49.9324	-0.5338	-0.0027	27.0193	0.1643	-0.0014
2	0.0000	-0.6570	0.0000	124.5024	0.0000	0.0000
3	49.9324	-0.5338	0.0027	27.0193	-0.1643	-0.0014
4	0.0	0.0	0.0000	0.0	0.0000	-0.0014

Note: suffices n and t refer to normal and tangential modes respectively.

Table 2: Side displacements of cantilever in Figure 3.

This raises the question: what is its optimum position? To give quantitative information on this question, strain energies are compared due to single traction modes and those combinations of tractions which lead to maximum and minimum energies. The ratio of the latter two values (eigenvalues) give a condition number for a flexibility matrix. These are compared for the full matrix $\left[F\right]$, and for the $(9\text{x}9)$ submatrix $\left[F^{bb}\right]$ which contains only those coefficients corresponding to "basic" loads and displacements. Traction modes or loads are termed "basic" for those with a resultant, and "higher order" for those which are self balancing along a side. For flexibility matrices an element is assumed to be supported on the side between nodes 4 and 1, so that the basic loads on this side are not independent. From a number of examples studied it is generally observed that

(a) strain energies due to basic loads, and the condition number of $\left[F^{bb}\right]$ are relatively insensitive to the position of node5.

b) strain energies due to higher order loads (particularly the quadratic modes), and the condition number of $\left[F\right]$ are relatively sensitive to the position of node 5.

c) for the general parallelogram shape of element, the diagonals intersect at the "isoparametric" centre, and the condition number of $\left[F\right]$ is minimum when node 5 is positioned there.

d) for a distorted element with taper the intersection D of the diagonals separates from the isoparametric centre, but the condition number of $\left[F\right]$ may reach a minimum with node 5 at neither of these positions.

These points are illustrated with two examples in Figures 4(a) and (b) where variations of energies and condition numbers with the position of node 5 are shown on a log scale. The strain energies have been normalised to unity for node 5 at the isoparametric centre. It should also be noted that for the tapered element the graphs have points of singularity when node 5 occurs at D, which coincides with the presence of an internal spurious kinematic mode.

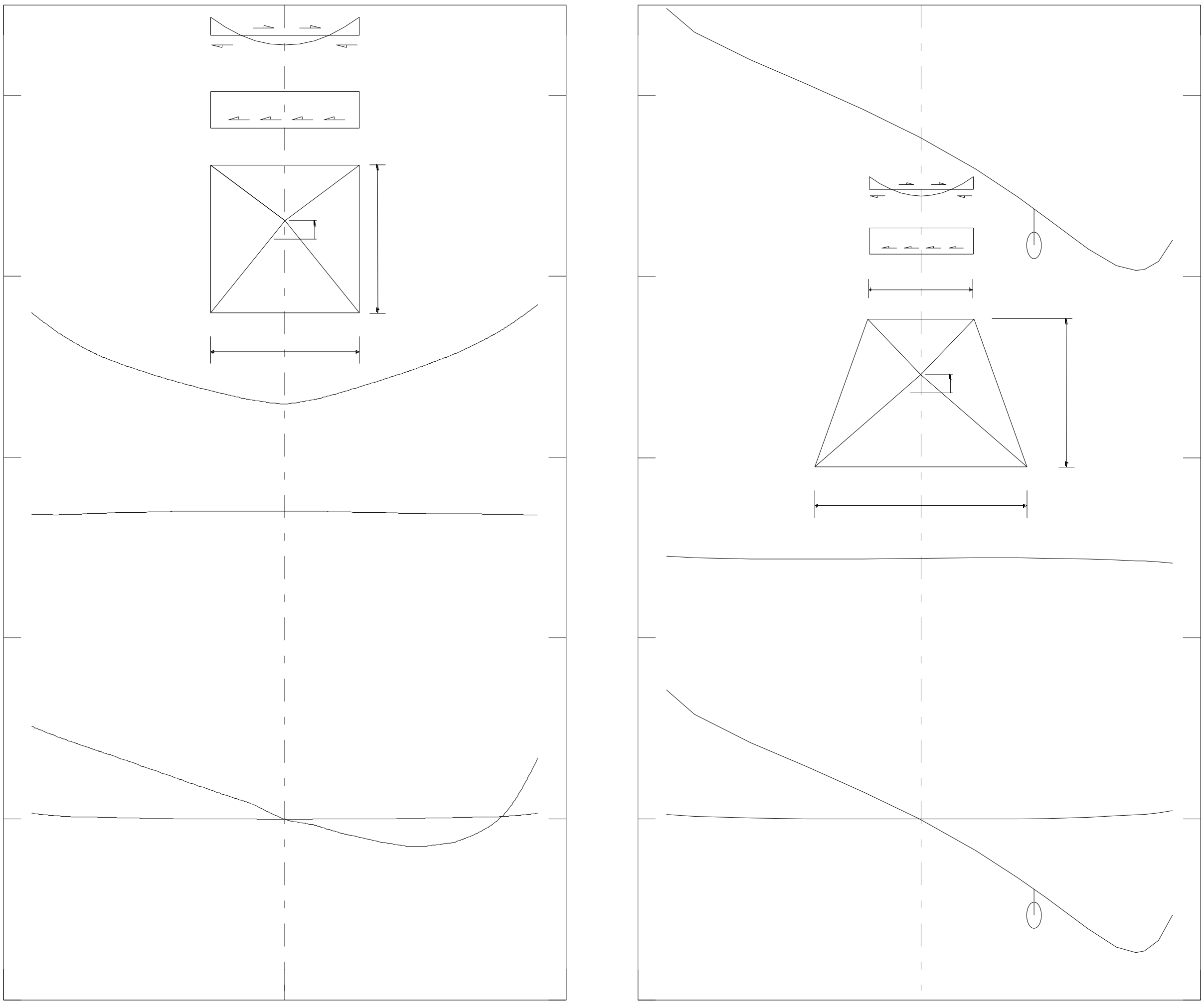

(a) Square element. (b) Tapered element.

Note: elements are supported on the side between nodes 4 and 1.

Figure 4: Element energies and condition numbers as functions of position of the internal node.

6. CONCLUSIONS.

1) It is considered that an efficient formulation of the superelement stress fields, and a flexibility matrix, have been achieved based on a force method of analysis. The element has no spurious kinematic modes EXCEPT when the internal subdivision uses the diagonals of the quadrilateral. This property appears to be the direct opposite to that used by Sander [2] for the original form of this element. However it remains true to say that when diagonals are used, the spurious mode is not excited by tractions applied to the sides of the element.

2) The element returns the correct response to tractions, independently of its subdivision, when the response entails compatible quadratic stress fields without body forces. However solutions with high strain energies can occur when higher order traction modes are applied such as would produce singularities in analytic solutions. The level of energy is then sensitive to the geometry of the internal subdivision. Further research is necessary to determine the significance of

such energies in multi-element models, which as equilibrium models provide upper bounds to total strain energies for force driven problems. This research should also address further the determination of optimum subdivision. It may yet emerge that diagonal subdivision is to be preferred.

7. REFERENCES.

1) FRAEIJS DE VEUBEKE, B.M., Displacement and equilibrium models in the finite element method. Chapter 9 in Stress Analysis, ed. by Zienkiewicz, O.C. and Holister, G.S., Wiley, 1965.

2) SANDER, G., Application of the dual analysis principle. pp.167-207 in High Speed Computing of Elastic Structures, ed. by Fraeijs de Veubeke B.M., Les Congres et Colloques de l'Universite de Liege, Vol. 61, 1971.

3) ROBINSON, J., The Mode Amplitude Technique and Hierarchical Stress Elements - A Simplified and Natural Approach. Int.J.Num.Meth.in Eng. Vol.21, pp.487-507, 1985.

4) MOITINHO DE ALMEIDA, J.P., and TEIXEIRA DE FREITAS, J.A., Alternative approach to the formulation of hybrid equilibrium finite elements. Computers and Structures, Vol.40, No.4, pp.1043-1047, 1991.

5) MAUNDER, E.A.W., A reappraisal of compound equilibrium finite elements. pp.796-797 in Proc.12th.Canadian Congress of Applied Mechanics, ed. by Erki,M.A. and Kirkhope,J. Vol.2, Carleton University, Ottawa, 1989.

6) LADEVEZE, P., PELLE, J.-P., and ROUGEOT, P., Error estimation and mesh optimization for classical finite elements. Engineering Computations, Vol.8, pp.69-80, 1991.

7) MAUNDER, E.A.W., and HILL, W.G., Complementary use of displacement and equilibrium models in analysis and design. pp.493-501 in FEM in the Design Process, ed. by Robinson,J., Robinson and Associates, 1990.

8) MAUNDER, E.A.W., Finite element modelling of Exeter Cathedral. Finite Element News, Issue No. 6, pp.14-18, 1991.

9) TEMIN-GENDRON,P.,and LAURENT-GENGOUX,P., Calculation of limit loads for composite materials via equilibrium finite elements. Computers and Structures, Vol.45, No.5/6, pp. 947-957, 1992.

10) FRAEIJS DE VEUBEKE, B.M., Matrix Structural Analysis. pp.509-567 in B.M. Fraeijs de Veubeke Memorial Volume of Selected Papers, ed. by Geradin,M., Sijthoff and Noordhoff/Waterloo University, 1980.

11) ARGYRIS, J. and MLEJNEK, H.-P., Die Methode der finiten Elemente, Band 1, Vieweg-Verlag, Braunschweig, 1986.

12) ROBINSON, J., Timoshenko's Beam Solutions Revisited - Membrane Educational Project. pp.262-270 in FEM in the Design Process, ed. by Robinson,J., Robinson and Associates, 1990.